Association of Retinal Microvasculature With Myopia Progression in Children: The Hong Kong Children Eye Study

Zi Xuan Lin,[1] Xiu Juan Zhang,[1,2] Fang Yao Tang,[1] Yuzhou Zhang,[1] Ka Wai Kam,[1,3] Alvin L. Young,[1,3] Patrick Ip,[4] Carol Y. Cheung,[1] Chi Pui Pang,[1,5,6] Clement C. Tham,[1,3,5–7,9] Li Jia Chen,[1,2,5,6] Kyoko Ohno-Matsui,[8] and Jason C. Yam[1,3,5–7,9]

[1]Department of Ophthalmology and Visual Sciences, The Chinese University of Hong Kong, Hong Kong
[2]Department of Ophthalmology, The University of Hong Kong, Hong Kong
[3]Department of Ophthalmology and Visual Sciences, Prince of Wales Hospital, Hong Kong
[4]Department of Paediatrics and Adolescent Medicine, University of Hong Kong, Hong Kong
[5]Joint Shantou International Eye Center of Shantou University and The Chinese University of Hong Kong, Shantou, China
[6]Hong Kong Hub of Paediatric Excellence, The Chinese University of Hong Kong, Hong Kong
[7]Hong Kong Eye Hospital, Hong Kong
[8]Department of Ophthalmology and Visual Science, Tokyo Medical and Dental University, Tokyo, Japan
[9]Department of Ophthalmology, Hong Kong Children's Hospital, Hong Kong

Correspondence: Jason C. Yam, Department of Ophthalmology and Visual Sciences, The Chinese University of Hong Kong, Hong Kong Eye Hospital, 147K Argyle Street, Kowloon, Hong Kong SAR 999077, China; yamcheuksing@cuhk.edu.hk.

ZXL and XJZ contributed equally to this work and should be considered co-first authors.

Received: December 16, 2024
Accepted: March 27, 2025
Published: April 22, 2025

Citation: Lin ZX, Zhang XJ, Tang FY, et al. Association of retinal microvasculature with myopia progression in children: The Hong Kong children eye study. *Invest Ophthalmol Vis Sci.* 2025;66(4):64. https://doi.org/10.1167/iovs.66.4.64

Purpose. To investigate the associations between optical coherence tomography angiography (OCT-A) metrics and myopia progression in children.

Methods. This prospective, longitudinal cohort study recruited children ages 6 to 8 years for 2- to 6-year follow-ups. OCT-A captured macular images from the superficial capillary plexus (SCP) and deep capillary plexus (DCP). Annual progression of spherical equivalent (SE) and axial length (AL) was calculated as (SE/AL at last visit – SE/AL at baseline)/follow-up duration. Multivariable linear regression analysis evaluated the associations of OCT-A metrics with SE/AL progression. Restricted cubic spline (RCS) analysis evaluated both linear and nonlinear associations. Holm–Bonferroni correction was applied to account for multiple comparisons.

Results. A total of 920 children were analyzed. Multivariable linear regression, adjusted for age, sex, baseline SE/AL, and other covariates, showed that baseline foveal avascular zone (FAZ) circularity was negatively associated with annual AL elongation ($\beta = -0.06$; 95% confidence interval [CI], −0.10 to −0.02; adjusted $P = 0.045$). Similarly, the baseline FAZ circularity was positively associated with annual SE progression ($\beta = 0.15$; 95% CI, 0.05–0.26; adjusted $P = 0.045$). No significant associations were found between OCT-A metrics in the DCP with annual AL/SE progression. Furthermore, RCS analysis demonstrated no significant nonlinear associations between OCT-A metrics and annual AL/SE progression (P for nonlinearity > 0.05).

Conclusions. Baseline FAZ circularity in the SCP was significantly associated with annual AL elongation and annual SE progression in children, suggesting its potential as an imaging biomarker for monitoring myopia progression.

Keywords: myopia, OCT-A, retinal microvasculature

Myopia affects millions of people worldwide. The prevalence of myopia in children 6 to 18 years old increased from 25% in 2000 to 41.9% in 2020 and is projected to reach 57.7% by 2050.[1] In some regions, particularly in East Asia, myopia has become a major public health concern with a high prevalence rate. Myopic individuals can develop ocular complications such as glaucoma, cataracts, retinal detachment, and myopic macular degeneration (MMD), which can lead to irreversible vision impairment and even blindness in patients with high myopia.[2] It is suggested that rapid myopic progression in childhood is associated with teenage high myopia.[3] Therefore, early detection and intervention are crucial to prevent or slow down myopia progression in children.

Optical coherence tomography angiography (OCT-A) provides an objective and non-invasive method to assess retinal microvasculature and the microvascular changes that can be associated with early-stage ocular diseases. OCT-A innovations have simplified the visualization and measurement of retinal microvasculature, without the requirement for exogenous intravenous dye injection.[4,5] The OCT-A metrics have been shown to be related to various microvascular abnormalities, including diabetic retinopathy,[6,7] retinal veinous occlusion,[8] and glaucoma.[9] Significantly, alterations in the

retinal microvasculature can be detected at a preclinical stage. This is evident in diabetic patients who show no signs of clinical retinopathy[10,11] and in those with glaucoma prior to visual field impairment.[12,13] Thus, OCT-A has proven effective in identifying early pathological changes within the retinal microvasculature. Certain characteristics within the retinal microvasculature observable through OCT-A scans may manifest before the emergence of significant retinal damage in children with myopia. Detecting these characteristics holds the potential for forecasting the progression of myopia and preventing visual impairment into the later teenage years and adulthood. Nevertheless, the association of OCT-A metrics with myopic progression in children has yet to be thoroughly investigated. Our study intended to assess the relationship between OCT-A metrics and the progression of myopia in children, utilizing data from the ongoing longitudinal Hong Kong Children Eye Study (HKCES) cohort.

Methods

Study Participants

This longitudinal, prospective study was conducted at the Hong Kong Eye Centre, The Chinese University of Hong Kong. Participants were a randomly selected subpopulation of the HKCES, a population-based cohort study on eye and vision conditions of ethnic Chinese children 6 to 8 years old. Each child underwent thorough physical and ophthalmological assessments at baseline and during subsequent visits, following protocols detailed elsewhere.[14] Children with retinal diseases, intraocular inflammation, histories of eye surgery, or systemic conditions that affect retinal microvasculature were excluded. The median follow-up duration of this study was 44 months, with a range from 27 to 82 months. To account for variations in follow-up duration, the total change in spherical equivalent (SE)/axial length (AL) was divided by each participant's follow-up duration to calculate the annual progression rate.[3,15]

This study adhered to the tenets of the Declaration of Helsinki, and the protocol of the study was approved by the ethics committee board of the Prince of Wales Hospital, The Chinese University of Hong Kong. Written informed consent was obtained from all parents or guardians, and verbal consent was additionally acquired from each child participant through age-appropriate explanation of study procedures prior to commencement of the study.

OCT-A Imaging and Quality Control

The methodology for OCT-A imaging and subsequent analysis adhered to previously established protocols.[16] In brief, OCT-A imaging uses swept-source OCT (DRI OCT Triton; Topcon, Tokyo, Japan) to obtain volumetric OCT scans encompassing a 6 × 6-mm grid with 320 × 320 A-scans centered on the fovea. This process captures OCT-A images from both the superficial capillary plexus (SCP) and the deep capillary plexus (DCP). The built-in IMAGEnet6 software provides a quality score ranging from 0 to 100 for each scan, with an established image quality threshold of ≥40 to proceed with further analysis.[16] OCT-A images were meticulously evaluated by two experienced readers (ZL, XZ) at The Chinese University of Hong Kong Ocular Reading Centre who were blinded to participant information to guarantee an impartial assessment. The exclusion criteria for artifacts of OCT-A images were established previously[16] and included the following: (1) OCT-A images with quality score < 40; (2) motion artifacts (e.g., discontinued vessels, residual motion lines); (3) segmentation errors in layers or slabs; (4) blurring images from media opacity or axial movement; (5) signal loss by blinking; or (6) foveal decentration (e.g., fovea not presented at the center of the image).

Quantification of Retinal Microvasculature

An established automated MATLAB 2017 program (MathWorks, Natick, MA, USA) was utilized for quantification of the OCT-A images. The process of image quantification, along with the evaluation of its reliability, has been described previously.[6] The Figure illustrates the quantification method used for OCT-A metrics within the SCP and DCP. Briefly, the area of the foveal avascular zone (FAZ) was calculated by counting the total number of pixels within the region in scale. FAZ circularity, reflecting the geometric regularity of FAZ, ranged from 0 (irregular shape) to 1 (nearly circular).[17] The non-perfusion areas (NPAs) were defined as regions with flow signals below 1.2 standard deviations above the mean decorrelation signal within the FAZ.[18] Vessel density (VD) was calculated as the percentage of perfused area, excluding the central 1-mm circle.

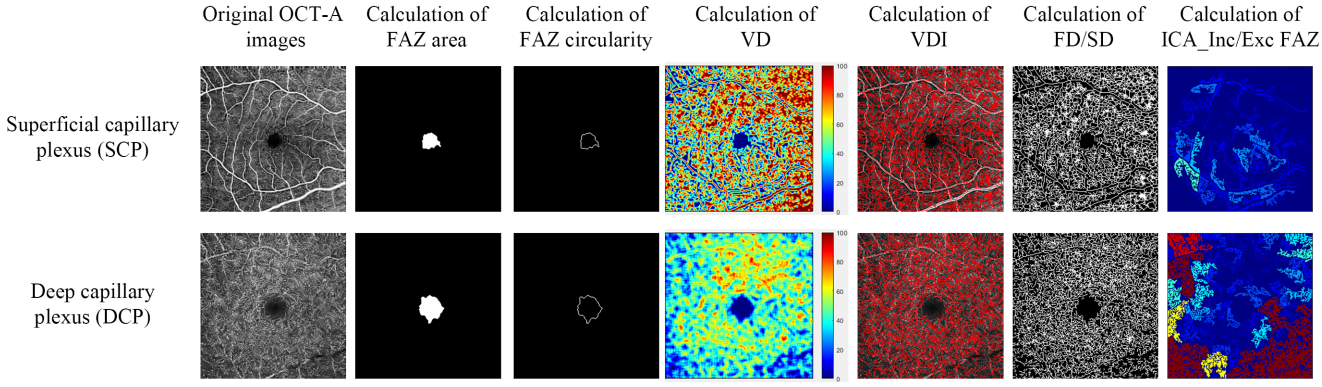

Figure. Quantification of the retinal capillary network from OCT-A images of the superficial capillary plexus and deep capillary plexus.

The binarized OCT-A image was further skeletonized to compute the skeleton density (SD), also known as the vessel length density (VLD), which represents the length of the blood vessel (pixels/pixels2),[19] and the fractal dimension (FD),[20] which delineates the vessel branching complexity. The vessel diameter index (VDI) was determined by dividing the vessel area by the total vessel length in the skeletonized image.[21] The intercapillary area (ICA) was quantified by identifying connected dark regions within the parafoveal area. ICA10_IncFAZ represents the top 10 largest dark areas, including the FAZ, and ICA10_ExcFAZ represents the top 10 largest dark areas, excluding the FAZ.[22] According to the Bennett–Littman method, the relationship between the measured swept-source OCT image and its actual size is given by the equation $t = 3.393 \times 0.01306(AL - 1.82) \times s$, where t is the actual size and s is the measured size. As a result, the actual sizes of the Early Treatment Diabetic Retinopathy Study (ETDRS) grids were adjusted to account for AL-related transverse magnification effects accordingly.[23,24]

Ophthalmic and Physical Examinations

Participants underwent a full ophthalmic examination. Cycloplegic autorefraction was conducted using an autorefractor (ARK-510A; Nidek, Aichi, Japan). The SE was calculated as the sum of the sphere power (diopters [D]) with half of the cylinder power (D). AL and the anterior chamber depth were measured with a ZEISS IOLMaster (Carl Zeiss Meditec, Jena, Germany). Intraocular pressure and central cornea thickness were measured with a tonometer (Corvis ST; OCULUS, Wetzlar, Germany). Macular thickness and macular volume were measured with the SPECTRALIS HRA+OCT (Heidelberg Engineering, Heidelberg, Germany). Progressive myopia was categorized as either progressive SE change ≤ -0.5 D per year[25] or progressive AL elongation ≥ 0.38 mm per year.[26] The annual SE/AL progression over the follow-up period was calculated as (SE/AL at last visit – SE/AL at baseline)/follow-up duration (year).[3,15]

A comprehensive physical examination was conducted on all participants. Heights and weights were measured using Seca (Hamburg, Germany) medical measuring systems and scales. Blood pressure and heart rate were measured using an automatic blood pressure monitor (Spacelabs Medical, Issaquah, WA, USA). Head and waist circumferences were measured using an anthropometric tape, and body mass index was calculated as weight (kg) divided by the square of height (m^2).

Sample Size

A previous study reported that the proportion of children with SE progression > -0.50 D per year who were ages 4 to 6 years was 20.5%, and the proportion in those 7 to 9 years old was 33.1%.[25] In this study, we used logistic regression analysis, assuming a type 1 error of 0.05% and a 20% loss to follow-up, to calculate a minimal sample size of 897 with sufficient power to detect an odds ratio of 1.5 for the association between incident progressive myopia and a range of exposures in this cohort. The sample size calculations were performed using G*Power 3.1.9.7.[27]

Statistical Analysis

All statistical analyses were performed using Stata 17 (StataCorp, College Station, TX, USA). Baseline differences between included and excluded participants were assessed using independent-samples t-tests or χ^2 tests (for categorical variables). Due to the skewed distribution of OCT-A metrics, a logarithmic transformation was applied to normalize the data. Given the narrow range and small deviation of FDs, we further applied z-score standardization to improve the numerical stability in the regression analysis. The OCT-A image of the right eye of each participant was used in the analysis; if the right eye image was excluded, the OCT-A image of the left eye was used instead. Univariable and multivariable linear regression analyses that adjusted for age, sex, baseline SE/AL, and potential covariates were carried out to investigate the correlations between baseline OCT-A metrics and the annual progression rate of SE and AL. Logistic regression analysis explored the relationship between baseline OCT-A metrics and progressive SE/AL changes. Three logistic regression models were constructed. Model 1 was unadjusted baseline OCT-A metrics, model 2 adjusted each metric for age and sex, and model 3 further adjusted for baseline SE/AL and potential covariates. The potential covariates adjusted for each OCT-A metrics were determined by univariable and multivariable linear regression analysis, as detailed in Supplementary Tables S1 to S4. For each analysis, both two-tailed unadjusted P values and Holm–Bonferroni corrected P values were provided to control the family-wise error rate. Restricted cubic spline (RCS) analysis was conducted to evaluate both the linear and nonlinear relationships between OCT-A metrics and annual AL/SE progression. A threshold of 0.05 was considered statistically significant across all analyses.

Results

Study Participants

A total of 1151 children were initially recruited for this study, and 143 children were excluded due to the low quality of OCT-A images at baseline. During the follow-up period, 88 children were lost to follow-up, resulting in a final cohort of 920 children included in the current study. The mean baseline age was 7.63 ± 1.01 years, with a mean baseline SE of 0.20 ± 1.37 D and a mean AL of 23.14 ± 0.89 mm. Over the follow-up period, progressive SE changes occurred in 325 children (35.32%), and progressive AL elongation was observed in 182 children (19.78%). Baseline demographic and ocular biometric data for the participants are detailed in Table 1.

Associations of OCT-A Metrics With Annual Myopia Progression

In the SCP, the multivariable linear regression analysis demonstrated a significant positive association between baseline FAZ area and annual AL elongation ($\beta = 0.03$; 95% confidence interval [CI], 0.004–0.06; $P = 0.03$). In contrast, FAZ circularity ($\beta = -0.06$; 95% CI, −0.10 to −0.02; $P = 0.01$) and FD ($\beta = -0.01$; 95% CI, −0.02 to 0.00; $P = 0.04$) exhibited significant negative associations with annual AL elongation before Holm–Bonferroni correction. However, after the Holm–Bonferroni correction, only the association of FAZ circularity remained statistically significant (adjusted $P = 0.045$) (Table 2). When assessing relationships between baseline OCT-A metrics and annual SE progression, baseline FAZ area showed a significant negative association ($\beta = -0.09$; 95% CI, −0.16 to −0.01; $P = 0.02$),

Table 1. Baseline Demographics and Ocular Characteristics of Participants

Variables	Excluded Subjects (n = 231)	Included Subjects (n = 920)	P
Male, n (%)	118 (51)	457 (49)	0.70
Age (y), mean ± SD	7.74 ± 1.10	7.63 ± 1.01	0.12
Blood pressure (mmHg), mean ± SD			
Systolic	104.58 ± 11.87	102.92 ± 11.34	0.05
Diastolic	65.97 ± 7.91	65.59 ± 8.07	0.52
Heart rate (bpm), mean ± SD	79.42 ± 11.19	79.61 ± 11.57	0.82
Body mass index (kg/m^2), mean ± SD	16.14 ± 2.47	16.16 ± 2.99	0.92
Waist circumference (cm), mean ± SD	58.43 ± 6.91	57.76 ± 6.62	0.17
Head circumference (cm), mean ± SD	51.96 ± 1.89	51.94 ± 1.87	0.85
Follow-up duration (mo), median (range)	—	44 (27–82)	—
Spherical equivalent (D), mean ± SD	−0.21 ± 1.93	0.20 ± 1.37	**<0.001**[*]
Axial length (mm), mean ± SD	23.28 ± 0.99	23.14 ± 0.89	**0.03**[*]
Anterior chamber depth (mm), mean ± SD	3.56 ± 0.26	3.56 ± 0.23	0.77
Central corneal thickness (µm), mean ± SD	548.76 ± 29.13	550.78 ± 32.54	0.40
Intraocular pressure (mmHg), mean ± SD	15.87 ± 2.75	15.68 ± 2.62	0.33
Visual acuity (logMAR), mean ± SD	0.13 ± 0.26	0.10 ± 0.24	0.17
Central macular thickness (µm), mean ± SD	245.59 ± 25.08	244.59 ± 27.00	0.62
Total macular volume (mm^2), mean ± SD	8.33 ± 0.64	8.24 ± 0.71	0.08
Average retinal nerve fiber layer thickness (µm), mean ± SD	101.79 ± 8.85	100.26 ± 8.86	**0.02**[*]

[*] Statistically significant P value ($P < 0.05$).

Table 2. Linear Regression Analysis for Superficial and Deep OCT-A Metrics With Annual AL Elongation

	Unadjusted				Adjusted[*]			
OCT-A Metrics (Log-Transformed)	β	95% CI	P	Adjusted P	β	95% CI	P	Adjusted P
Superficial Capillary Plexus								
FAZ area	0.03	−0.003 to 0.06	0.08	0.63	0.03	0.004 to 0.06	**0.03**[†]	0.20
FAZ circularity	−0.06	−0.10 to −0.01	**0.02**[†]	0.14	−0.06	−0.10 to −0.02	**0.01**[†]	**0.045**[‡]
VD	−0.07	−0.22 to 0.07	0.33	0.98	−0.08	−0.22 to 0.05	0.22	1.00
VDI	0.01	−0.10 to 0.12	0.82	1.00	0.07	−0.04 to 0.17	0.21	1.00
FD (standardized)	−0.01	−0.02 to 0.002	0.10	0.63	−0.01	−0.02 to 0.00	**0.04**[†]	0.30
SD	−0.02	−0.11 to 0.07	0.65	1.00	−0.05	−0.13 to 0.03	0.20	1.00
NPA	0.06	−0.01 to 0.12	0.09	0.63	0.03	−0.03 to 0.09	0.29	1.00
ICA10_IncFAZ	0.02	−0.01 to 0.05	0.15	0.77	0.02	−0.01 to 0.05	0.19	1.00
ICA10_ExcFAZ	0.02	−0.01 to 0.05	0.22	0.89	0.01	−0.01 to 0.04	0.32	1.00
Deep Capillary Plexus								
FAZ area	0.01	−0.02 to 0.04	0.42	1.00	0.02	−0.004 to 0.05	0.10	0.86
FAZ circularity	−0.03	−0.08 to 0.02	0.19	1.00	−0.04	−0.08 to 0.01	0.10	0.86
VD	0.002	−0.09 to 0.10	0.97	1.00	−0.01	−0.10 to 0.07	0.75	1.00
VDI	0.01	−0.16 to 0.17	0.95	1.00	0.06	−0.10 to 0.22	0.47	1.00
FD (standardized)	−0.003	−0.01 to 0.01	0.60	1.00	−0.004	−0.01 to 0.01	0.42	1.00
SD	0.00	−0.07 to 0.07	1.00	1.00	−0.02	−0.08 to 0.04	0.47	1.00
NPA	−0.01	−0.14 to 0.12	0.91	1.00	0.03	−0.09 to 0.15	0.62	1.00
ICA10_IncFAZ	0.01	−0.02 to 0.03	0.72	1.00	0.01	−0.02 to 0.04	0.42	1.00
ICA10_ExcFAZ	0.01	−0.02 to 0.03	0.69	1.00	0.01	−0.02 to 0.03	0.53	1.00

Note that the log-transformed FD was further standardized to improve numerical stability on the regression analysis.
[*] Adjusted for age, sex, baseline AL, and other covariates.
[†] Statistically significant P value before adjustment ($P < 0.05$).
[‡] P value that remained statistically significant after Holm–Bonferroni correction ($P < 0.05$).

whereas FAZ circularity demonstrated a significant positive association (β = 0.15; 95% CI, 0.05–0.26; P = 0.01) before Holm–Bonferroni correction. After Holm–Bonferroni correction, only FAZ circularity remained statistically significant (adjusted P = 0.045) (Table 3). However, no significant associations were observed between OCT-A metrics within the DCP and the annual progression of AL/SE (Tables 2, 3). In the univariable and multivariable analyses on the associations of VD in different parafoveal sectors, we found no significant associations with annual AL elongation or annual SE progression across the SCP and DCP (Table 4).

Dose–Response Relationships of OCT-A Metrics With Annual Myopia Progression

RCS analysis with all covariates adjusted was conducted to evaluate the linear or nonlinear relationships between the OCT-A metrics and annual AL/SE progression. Overall, none of the OCT-A metrics demonstrated significant nonlinear associations with annual AL/SE progression in both SCP and DCP (Supplementary Figs. S2–S5). Supplementary Figure S2 shows restricted cubic splines indicating dose–response linear relationships of the FAZ area (P

Table 3. Linear Regression Analysis for Superficial and Deep OCT-A Metrics With Annual SE Progression

	Unadjusted				Adjusted*			
OCT-A Metrics (Log-Transformed)	**β**	**95% CI**	***P***	**Adjusted *P***	**β**	**95% CI**	***P***	**Adjusted *P***
Superficial Capillary Plexus								
FAZ area	−0.08	−0.15 to −0.004	**0.04**†	0.31	−0.09	−0.16 to −0.01	**0.02**†	0.16
FAZ circularity	0.14	0.03 to 0.25	**0.01**†	0.11	0.15	0.05 to 0.26	**0.01**†	**0.045**‡
VD	0.08	−0.27 to 0.44	0.64	1.00	0.10	−0.24 to 0.44	0.57	1.00
VDI	0.07	−0.20 to 0.33	0.62	1.00	0.01	−0.25 to 0.27	0.93	1.00
FD (standardized)	0.02	−0.01 to 0.05	0.23	1.00	0.02	−0.01 to 0.05	0.20	1.00
SD	−0.02	−0.23 to 0.19	0.86	1.00	0.02	−0.19 to 0.22	0.85	1.00
NPA	−0.08	−0.24 to 0.08	0.33	1.00	−0.04	−0.19 to 0.12	0.62	1.00
ICA10_IncFAZ	−0.01	−0.08 to 0.06	0.79	1.00	−0.01	−0.08 to 0.06	0.79	1.00
ICA10_ExcFAZ	0.00	−0.07 to 0.07	0.99	1.00	0.001	−0.06 to 0.07	0.96	1.00
Deep Capillary Plexus								
FAZ area	−0.02	−0.08 to 0.05	0.58	1.00	−0.05	−0.12 to 0.01	0.11	0.91
FAZ circularity	0.07	−0.05 to 0.19	0.24	1.00	0.11	−0.01 to 0.22	0.07	0.62
VD	−0.11	−0.34 to 0.12	0.35	1.00	−0.11	−0.33 to 0.12	0.34	1.00
VDI	0.09	−0.32 to 0.49	0.67	1.00	0.03	−0.37 to 0.43	0.88	1.00
FD (standardized)	0.00	−0.03 to 0.03	0.98	1.00	−0.001	−0.03 to 0.03	0.93	1.00
SD	−0.07	−0.22 to 0.09	0.42	1.00	−0.05	−0.20 to 0.11	0.57	1.00
NPA	0.06	−0.26 to 0.37	0.73	1.00	0.07	−0.23 to 0.38	0.63	1.00
ICA10_IncFAZ	0.01	−0.06 to 0.08	0.78	1.00	0.01	−0.06 to 0.07	0.81	1.00
ICA10_ExcFAZ	0.01	−0.06 to 0.07	0.85	1.00	0.02	−0.04 to 0.07	0.63	1.00

Note that the log-transformed FD was further standardized to improve numerical stability on the regression analysis.
* Adjusted for age, sex, baseline SE, and other covariates.
† Statistically significant *P* value before adjustment ($P < 0.05$).
‡ *P* value that remained statistically significant after Holm–Bonferroni correction ($P < 0.05$).

Table 4. Linear Regression Analysis for Superficial and Deep VD in Parafoveal Sectors With Annual Myopia Progression

	Unadjusted				Adjusted*			
OCT-A Metrics (Log-Transformed)	**β**	**95% CI**	***P***	**Adjusted *P***	**β**	**95% CI**	***P***	**Adjusted *P***
Annual AL Elongation								
Superficial VD in parafoveal sectors								
Superior VD	−0.07	−0.18 to 0.05	0.27	0.82	−0.04	−0.15 to 0.07	0.45	1.00
Inferior VD	0.00	−0.07 to 0.07	0.98	1.00	−0.02	−0.08 to 0.05	0.59	1.00
Temporal VD	0.02	−0.08 to 0.12	0.70	1.00	−0.03	−0.13 to 0.06	0.52	1.00
Nasal VD	−0.05	−0.11 to 0.02	0.20	0.78	−0.02	−0.08 to 0.05	0.62	1.00
Deep VD in parafoveal sectors								
Superior VD	0.01	−0.06 to 0.07	0.85	1.00	0.03	−0.03 to 0.08	0.39	1.00
Inferior VD	0.01	−0.02 to 0.04	0.73	1.00	0.00	−0.03 to 0.03	0.97	1.00
Temporal VD	0.04	−0.02 to 0.10	0.18	0.71	0.02	−0.04 to 0.07	0.57	1.00
Nasal VD	−0.03	−0.08 to 0.02	0.23	0.71	−0.01	−0.06 to 0.03	0.55	1.00
Annual SE Progression								
Superficial VD in parafoveal sectors								
Superior VD	0.22	−0.07 to 0.50	0.13	0.53	0.18	−0.09 to 0.46	0.19	0.75
Inferior VD	−0.10	−0.26 to 0.07	0.26	0.77	−0.06	−0.23 to 0.10	0.43	1.00
Temporal VD	−0.01	−0.26 to 0.24	0.96	1.00	0.10	−0.14 to 0.34	0.43	1.00
Nasal VD	0.04	−0.13 to 0.20	0.67	1.00	−0.03	−0.19 to 0.13	0.68	1.00
Deep VD in parafoveal sectors								
Superior VD	−0.05	−0.20 to 0.10	0.52	1.00	−0.08	−0.23 to 0.06	0.26	0.79
Inferior VD	−0.05	−0.12 to 0.02	0.14	0.57	−0.05	−0.12 to 0.02	0.18	0.72
Temporal VD	−0.08	−0.22 to 0.07	0.30	0.89	−0.07	−0.21 to 0.07	0.32	0.79
Nasal VD	0.01	−0.11 to 0.12	0.94	1.00	−0.03	−0.14 to 0.09	0.62	0.79

* Adjusted for age, sex, baseline AL/SE, and other covariates.

for overall = 0.04; *P* for nonlinear = 0.20) and FAZ circularity (*P* for overall = 0.003; *P* for nonlinear = 0.05) with annual AL progression. Additionally, FAZ circularity (*P* for overall = 0.01; *P* for nonlinear = 0.20) demonstrated a dose–response linear association with annual SE progression (Supplementary Fig. S3).

Associations of OCT-A Metrics With Progressive Myopia

Apart from linear regression, an exploratory logistic regression analysis was conducted to assess the relationship between the OCT-A metric and progressive or non-

progressive myopia. Supplementary Table S5 shows that all baseline OCT-A metrics in the SCP were significantly associated with progressive AL elongation in model 3 ($P < 0.05$). However, no significant associations were found in the OCT-A metric with progressive SE changes in either the SCP and DCP (Supplementary Table S6). Similarly, no significant associations were found in the association of sectoral VD and progressive AL/SE change. (Supplementary Table S7).

Discussion

Our study revealed a significant negative association between baseline FAZ circularity in the SCP and annual AL elongation, as well as a significant positive association with annual SE progression. Restricted cubic splines demonstrated no significant nonlinearity between baseline OCT-A metrics and annual myopia progression. These findings suggest that baseline FAZ circularity in the SCP may serve as a valuable imaging biomarker for monitoring myopia progression in children.

Previous research has primarily applied OCT-A to evaluate retinal microvascular changes in a variety of eye diseases[6–9] and across different degrees of myopia,[28–31] but they were predominantly cross-sectional and did not address longitudinal changes. Few studies have explored the relationship between OCT-A metrics and longitudinal myopia progression in children. Our findings align with emerging evidence suggesting that OCT-A can detect microvascular alterations before clinical symptoms emerge.[32,33] Although the exact mechanisms linking retinal microvasculature and myopia progression remain unclear, several studies have suggested that structural changes in myopic eyes, such as axial elongation, may lead to retinal stretching and thinning, altering retinal blood flow and vessel morphology.[34,35] Zhang et al.[26] reported that children with a rapid myopia progression trajectory face an elevated risk of developing MMD and having poorer best-corrected visual acuity. It is plausible that mechanical stress disrupts the retinal microvascular network, reducing retinal perfusion, especially in the foveal region. Because the fovea is critical for central vision, disruptions to its blood supply could impair visual acuity and stimulate compensatory growth of the eye to improve focus.[36]

The FAZ located in the central fovea is a region devoid of blood vessels that plays a crucial role in maintaining visual acuity. Its dimensions and morphology can be quantified using OCT-A metrics such as FAZ area and FAZ circularity. The FAZ area measures the size of the avascular zone, and the FAZ circularity reflects how closely its shape approximates a perfect circle. Several studies have reported a significantly enlarged FAZ area in highly myopic eyes for both the SCP and DCP.[37–41] Additionally, reduced FAZ circularity has been associated with parafoveal capillary network disruption and visual field defects in glaucoma patients,[42,43] as well as reduced visual function in diabetic retinopathy.[6] Although some studies have suggested that FAZ circularity is lower in myopic eyes compared to emmetropic eyes, their results have lacked statistical significance.[40,44,45] The association between FAZ circularity and longitudinal myopia progression remains unexplored. In the current study, we observed a dose-dependent negative association of FAZ circularity in the SCP and annual AL elongation, along with a positive association with annual SE progression. Our findings indicate that individuals with lower FAZ circularity in the SCP may experience a higher annual axial elongation and annual refractive error shift. These findings suggest that deviations from a more circular FAZ shape may reflect microvascular alterations associated with axial elongation, highlighting the potential of FAZ circularity as a biomarker for monitoring myopia progression.

In this study, a discrepancy was observed between the results the of linear regression and logistic regression analyses, with several OCT-A metrics exhibiting significant associations with myopia progression in the logistic regression but not in the linear regression. The logistic regression analysis was conducted as an exploratory analysis to gain insights into the association between OCT-A metrics and progressive and non-progressive myopia. Nevertheless, our restricted cubic spline analysis demonstrated an overall linear-like curve for the OCT-A metrics with annual myopia progression, with no significant nonlinearity (all P for nonlinear $>$ 0.05) (Supplementary Figs. S2–S5). This suggests that the discrepancy likely arose from the limited statistical power of the current sample size. A cohort study with a larger sample size is warranted to validate these preliminary findings and clarify the precise relationship between OCT-A metrics and myopia progression.

Interestingly, a more prominent association between OCT-A metrics and myopia progression was observed in the SCP than in the DCP. One plausible explanation for this is that the mechanical stretching and thinning of myopic eyes may affect different retinal layers, depending on their anatomical locations.[46,47] The SCP, extending from the nerve fiber layer to the ganglion cell layer, may be more susceptible to changes in ocular perfusion and biomechanical stress induced by axial elongation than the DCP. Additionally, the roles that each plexus may play in myopic changes may also contribute to these findings. During axial elongation, the mechanical stretching of the retina and choroid may impact the blood supply and decrease the oxygen and nutrient supply to the sclera, causing a hypoxia environment and increased energy demand.[48] The SCP more directly influences the inner retinal vasculature, and the DCP addresses the increased metabolic demands of the outer retina during rapid eye growth.[49] This increased metabolic activity may stimulate compensatory angiogenesis in the DCP before progressive myopia occurs, making it less sensitive to early axial changes.[50–52] Future studies with larger longitudinal cohorts and advanced OCT-A imaging techniques are necessary to better elucidate the differential roles of the SCP and DCP in myopia progression.

A key strength of our study is the longitudinal assessment of the baseline OCT-A metrics with myopia progression, compared to prior cross-sectional studies. Furthermore, the use of quantitative OCT-A metrics allowed a more precise characterization of retinal microvasculature. Our findings provide valuable insights into children's retinal vascular networks and their associations with myopia progression. However, it is important to acknowledge some limitations of this study. First, our study was observational, so it demonstrated associations but not causation between OCT-A metrics and myopia progression. Second, our study population consisted exclusively of ethnic Chinese children, which may limit the generalizability of our findings to other populations. Additional study in diverse populations is necessary to validate our findings. Finally, certain OCT-A metrics (e.g., FAZ area, VDI) showed statistical significance in the initial linear analysis, but their significance was lost after Holm–Bonferroni correction of the P values.

This suggests that some findings may be influenced by type I errors across multiple comparisons. Future studies with larger cohorts and advanced statistical modeling may help to better elucidate the clinical relevance of these OCT-A metrics.

In conclusion, our study highlights significant associations between the baseline FAZ circularity in the SCP and annual myopia progression in children. Detecting early signs of myopia progression is critical for facilitating timely interventions in children at risk of developing high myopia–related visual impairment. OCT-A holds great potential as a non-invasive imaging tool for identifying microvascular changes associated with myopia progression. Further research is warranted to unveil the underlying mechanisms and explore the clinical utility of OCT-A in the management of myopia.

Acknowledgments

Supported in part by the General Research Fund (GRF), Research Grants Council, Hong Kong (14102422 [JCY]); Collaborative Research Fund (C7149-20G [JCY]); Health and Medical Research Fund (HMRF), Hong Kong (11220206 [JCY], 10210246 [YZ], 09202466 [LJC]), National Natural Science Foundation of China (82425017 & 82171089 [JCY]); Strategic Impact Enhancement Fund, The Chinese University of Hong Kong (WW/SC/rc/SIEF2324/0366/24vw & TL/JF/rc/SIEF2223/0759/23vw [JCY]); the CUHK Jockey Club Children's Eye Care Programme (No grant number); and the CUHK Jockey Club Myopia Prevention Programme (No grant number).

Author Contributors: JCY, CPP, CCT, and LJC designed the study; ZXL and XJZ collected the data; ZXL and FYT analyzed and interpreted the data; KOM, FYT, YZ, KWK, ALY, PI, and CYC provided technical consultation. ZXL and XJZ drafted the manuscript; JCY, CPP, CCT, and LJC revised the manuscript.

Disclosure: **Z.X. Lin**, None; **X.J. Zhang**, None; **F.Y. Tang**, None; **Y. Zhang**, None; **K.W. Kam**, None; **A.L. Young**, None; **P. Ip**, None; **C.Y. Cheung**, None; **C.P. Pang**, None; **C.C. Tham**, None; **L.J. Chen**, None; **K. Ohno-Matsui**, None; **J.C. Yam**, None

References

1. Holden BA, Fricke TR, Wilson DA, et al. Global prevalence of myopia and high myopia and temporal trends from 2000 through 2050. *Ophthalmology*. 2016;123:1036–1042.
2. Saw SM, Gazzard G, Shih-Yen EC, Chua WH. Myopia and associated pathological complications. *Ophthalmic Physiol Opt*. 2005;25:381–391.
3. Lanca C, Foo LL, Ang M, et al. Rapid myopic progression in childhood is associated with teenage high myopia. *Invest Ophthalmol Vis Sci*. 2021;62:17.
4. Jia Y, Bailey ST, Hwang TS, et al. Quantitative optical coherence tomography angiography of vascular abnormalities in the living human eye. *Proc Natl Acad Sci USA*. 2015;112:E2395–E2402.
5. Spaide RF, Klancnik JM, Jr, Cooney MJ. Retinal vascular layers imaged by fluorescein angiography and optical coherence tomography angiography. *JAMA Ophthalmol*. 2015;133:45–50.
6. Tang FY, Ng DS, Lam A, et al. Determinants of quantitative optical coherence tomography angiography metrics in patients with diabetes. *Sci Rep*. 2017;7:2575.
7. Sun Z, Tang F, Wong R, et al. OCT angiography metrics predict progression of diabetic retinopathy and development of diabetic macular edema: a prospective study. *Ophthalmology*. 2019;126:1675–1684.
8. Kashani AH, Lee SY, Moshfeghi A, Durbin MK, Puliafito CA. Optical coherence tomography angiography of retinal venous occlusion. *Retina*. 2015;35:2323–2331.
9. Yarmohammadi A, Zangwill LM, Diniz-Filho A, et al. Optical coherence tomography angiography vessel density in healthy, glaucoma suspect, and glaucoma eyes. *Invest Ophthalmol Vis Sci*. 2016;57:OCT451–OCT459.
10. Arias JD, Arango FJ, Parra MM, et al. Early microvascular changes in patients with prediabetes evaluated by optical coherence tomography angiography. *Ther Adv Ophthalmol*. 2021;13:25158414211047020.
11. Li H, Yu X, Zheng B, Ding S, Mu Z, Guo L. Early neurovascular changes in the retina in preclinical diabetic retinopathy and its relation with blood glucose. *BMC Ophthalmol*. 2021;21:220.
12. Lee MY, Park HL, Kim SA, Jung Y, Park CK. Predicting visual field progression by optical coherence tomography angiography and pattern electroretinography in glaucoma. *J Glaucoma*. 2022;31:881–890.
13. Nishida T, Moghimi S, Wu JH, et al. Association of initial optical coherence tomography angiography vessel density loss with faster visual field loss in glaucoma. *JAMA Ophthalmol*. 2022;140:319–326.
14. Yam JC, Tang SM, Kam KW, et al. High prevalence of myopia in children and their parents in Hong Kong Chinese population: the Hong Kong Children Eye Study. *Acta Ophthalmol*. 2020;98:e639–e648.
15. Kong K, Jiang J, Wang P, et al. Progression patterns and risk factors of axial elongation in young adults with nonpathologic high myopia: three-year large longitudinal cohort follow-up. *Am J Ophthalmol*. 2024;267:293–303.
16. Cheung CY, Li J, Yuan N, et al. Quantitative retinal microvasculature in children using swept-source optical coherence tomography: the Hong Kong Children Eye Study [published online ahead of print June 28, 2018. *Br J Ophthalmol*, https://doi.org/10.1136/bjophthalmol-2018-312413.
17. Domalpally A, Danis RP, White J, et al. Circularity index as a risk factor for progression of geographic atrophy. *Ophthalmology*. 2013;120:2666–2671.
18. Hwang TS, Gao SS, Liu L, et al. Automated quantification of capillary nonperfusion using optical coherence tomography angiography in diabetic retinopathy. *JAMA Ophthalmol*. 2016;134:367–373.
19. Kim AY, Chu Z, Shahidzadeh A, Wang RK, Puliafito CA, Kashani AH. Quantifying microvascular density and morphology in diabetic retinopathy using spectral-domain optical coherence tomography angiography. *Invest Ophthalmol Vis Sci*. 2016;57:OCT362–OCT370.
20. Reif R, Qin J, An L, Zhi Z, Dziennis S, Wang R. Quantifying optical microangiography images obtained from a spectral domain optical coherence tomography system. *Int J Biomed Imaging*. 2012;2012:509783.
21. Wong TY, Kamineni A, Klein R, et al. Quantitative retinal venular caliber and risk of cardiovascular disease in older persons: the cardiovascular health study. *Arch Intern Med*. 2006;166:2388–2394.
22. Schottenhamml J, Moult EM, Ploner S, et al. An automatic, intercapillary area-based algorithm for quantifying diabetes-related capillary dropout using optical coherence tomography angiography. *Retina*. 2016;36(suppl 1):S93–S101.
23. Bennett AG, Rudnicka AR, Edgar DF. Improvements on Littmann's method of determining the size of retinal features by fundus photography. *Graefes Arch Clin Exp Ophthalmol*. 1994;232:361–367.
24. Deng J, Jin J, Zhang B, et al. Effect of ocular magnification on macular choroidal thickness measurements made

using optical coherence tomography in children. *Curr Eye Res*. 2022;47:1538–1546.
25. Tricard D, Marillet S, Ingrand P, Bullimore MA, Bourne RRA, Leveziel N. Progression of myopia in children and teenagers: a nationwide longitudinal study. *Br J Ophthalmol*. 2022;106:1104–1109.
26. Zhang S, Chen Y, Li Z, et al. Axial elongation trajectories in Chinese children and adults with high myopia. *JAMA Ophthalmol*. 2024;142:87–94.
27. Faul F, Erdfelder E, Buchner A, Lang AG. Statistical power analyses using G*Power 3.1: tests for correlation and regression analyses. *Behav Res Methods*. 2009;41:1149–1160.
28. Guo Y, Pang Y, Kang Y, et al. Correlations among peripapillary vasculature, macular superficial capillaries, and eye structure in healthy and myopic eyes of Chinese young adults (STROBE). *Medicine (Baltimore)*. 2020;99:e22171.
29. He J, Chen Q, Yin Y, et al. Association between retinal microvasculature and optic disc alterations in high myopia. *Eye (Lond)*. 2019;33:1494–1503.
30. Leng Y, Tam EK, Falavarjani KG, Tsui I. Effect of age and myopia on retinal microvasculature. *Ophthalmic Surg Lasers Imaging Retina*. 2018;49:925–931.
31. Li MY, Jin EZ, Dong CY, Zhang C, Zhao MW, Qu JF. The repeatability of superficial retinal vessel density measurements in eyes with long axial length using optical coherence tomography angiography. *BMC Ophthalmol*. 2018;18:326.
32. Vujosevic S, Toma C, Villani E, et al. Early detection of microvascular changes in patients with diabetes mellitus without and with diabetic retinopathy: comparison between different swept-source OCT-A instruments. *J Diabetes Res*. 2019;2019:2547216.
33. Wijesingha N, Tsai WS, Keskin AM, et al. Optical coherence tomography angiography as a diagnostic tool for diabetic retinopathy. *Diagnostics (Basel)*. 2024;14:326.
34. Gentle A, McBrien NA. Modulation of scleral DNA synthesis in development of and recovery from induced axial myopia in the tree shrew. *Exp Eye Res*. 1999;68:155–163.
35. Nickla DL, Wildsoet C, Wallman J. Compensation for spectacle lenses involves changes in proteoglycan synthesis in both the sclera and choroid. *Curr Eye Res*. 1997;16:320–326.
36. Wildsoet C, Wallman J. Choroidal and scleral mechanisms of compensation for spectacle lenses in chicks. *Vision Res*. 1995;35:1175–1194.
37. Sung MS, Lee TH, Heo H, Park SW. Association between optic nerve head deformation and retinal microvasculature in high myopia. *Am J Ophthalmol*. 2018;188:81–90.
38. Cheng D, Chen Q, Wu Y, et al. Deep perifoveal vessel density as an indicator of capillary loss in high myopia. *Eye (Lond)*. 2019;33:1961–1968.
39. Lee JH, Lee MW, Baek SK, Lee YH. Repeatability of manual measurement of foveal avascular zone area in optical coherence tomography angiography images in high myopia. *Korean J Ophthalmol*. 2020;34:113–120.
40. Piao HL, Guo Y, Zhang HW, Sung MS, Park SW. Acircularity and circularity indexes of the foveal avascular zone in high myopia. *Sci Rep*. 2021;11:16808.
41. Xu Q, Zhang W, Zhu H, Chen Q. Foveal avascular zone volume: a new index based on optical coherence tomography angiography images. *Retina*. 2021;41:595–601.
42. Kwon J, Choi J, Shin JW, Lee J, Kook MS. Alterations of the foveal avascular zone measured by optical coherence tomography angiography in glaucoma patients with central visual field defects. *Invest Ophthalmol Vis Sci*. 2017;58:1637–1645.
43. Choi J, Kwon J, Shin JW, Lee J, Lee S, Kook MS. Quantitative optical coherence tomography angiography of macular vascular structure and foveal avascular zone in glaucoma. *PLoS One*. 2017;12:e0184948.
44. Wang XQ, Xia LK. Effect of macular vascular density on visual quality in young myopic adults. *Front Med (Lausanne)*. 2022;9:950731.
45. Yao H, Xin D, Li Z. The deep vascular plexus density is closely related to myopic severity. *Ophthalmic Res*. 2022;65:455–465.
46. Zhao M, Lam AK, Cheong AM. Structural and haemodynamic properties of ocular vasculature in axial myopia. *Clin Exp Optom*. 2022;105:247–262.
47. Lin C, Toychiev A, Ablordeppey R, Slavi N, Srinivas M, Benavente-Perez A. Myopia alters the structural organization of the retinal vasculature, GFAP-positive glia, and ganglion cell layer thickness. *Int J Mol Sci*. 2022;23:6202.
48. Qi Z, Liu X, Xiong S, et al. Macular and peripapillary choroidal vascularity index in children with different refractive status. *Eye (Lond)*. 2024;38:606–613.
49. Ye J, Wang M, Shen M, et al. Deep retinal capillary plexus decreasing correlated with the outer retinal layer alteration and visual acuity impairment in pathological myopia. *Invest Ophthalmol Vis Sci*. 2020;61:45.
50. Chen P, Ji J, Chen X, Zhang J, Wen X, Liu L. Retinal glia in myopia: current understanding and future directions. *Front Cell Dev Biol*. 2024;12:1512988.
51. Medina-Arellano AE, Albert-Garay JS, Medina-Sanchez T, Fonseca KH, Ruiz-Cruz M, Ochoa-de la Paz L. Müller cells and retinal angiogenesis: critical regulators in health and disease. *Front Cell Neurosci*. 2024;18:1513686.
52. Quiroz-Reyes MA, Lima-Gomez V, eds. *Optical Coherence Tomography Angiography for Choroidal and Vitreoretinal Disorders – Part 2*. United Arab Emirates: Bentham Science Publishers; 2023.

Investigative Ophthalmology & Visual Science